Published in final edited form as:
Pain. 2009 February ; 141(3): 258–268. doi:10.1016/j.pain.2008.11.018.

Area-specific Representation of Mechanical Nociceptive Stimuli within SI Cortex of Squirrel Monkeys

Li Min Chen[1,2], **Robert M. Friedman**[3], and **Anna Wang Roe**[3]

1*Department of Radiology and Radiological Science, Vanderbilt University, Nashville, TN, 37203*

2*Institute of Imaging Science, Vanderbilt University, Nashville, TN, 37203*

3*Department of Psychology, Vanderbilt University, Nashville, TN, 37203*

Abstract

While functional imaging studies in humans have consistently reported activation of primary somatosensory cortex (SI) with painful stimuli, the specific roles of subdivisions of areas 3a, 3b and 1 within SI during pain perception are largely unknown, particularly in the representation of mechanical evoked pain. In this study, we investigated how modality, location, and intensity of nociceptive stimuli are represented within SI by using high-spatial resolution optical imaging of intrinsic signals in Pentothal-anesthetized squirrel monkeys. Perceptually comparable mechanical nociceptive and innocuous tactile stimuli were delivered by indenting the glabrous skin of the distal fingerpads with 0.2 and 2 mm diameter probes, respectively. Within each of areas 3a, 3b, and 1, activations to mechanical nociceptive stimulation of individual distal fingerpads were spatially distinct and somatotopically organized. We observed differential cortical activation patterns. Areas 3a, 3b and 1 were all activated during mechanical nociceptive stimulation and were modulated by nociceptive stimulus intensity. However, with innocuous tactile stimulation, mainly areas 3b and 1 exhibited response modulation with different levels of stimulation. In summary, mechanical nociceptive inputs are area-specific and topographically represented within SI. We propose that all areas of SI are implicated in encoding the features of mechanical nociception, where areas 3a and 3b are distinctively involved in coding nociceptive and pressure sensation components of stimulation.

Keywords

mechanical nociception; intrinsic optical imaging; primary somatosensory cortex; primate; digit; touch

Introduction

Advances in functional brain imaging techniques have led to the identification of possible neuroanatomical substrates of pain perception. Among them, cortical areas SI and SII (primary and second somatosensory cortices) have been proposed to play essential roles in the processing

Send Correspondence to: Li Min Chen MD, PhD, Department of Radiology and Radiological Science, Institute of Imaging Science, Vanderbilt University, 1161 21st Ave. S., Nashville, TN, 37232-2310, Tel: (615) 936-7069, Fax: (615) 322-0734, Email: E-mail: limin.chen@vanderbilt.edu.

We declare no conflict of interest in publishing this paper.

of the sensory-discriminative components of pain; these include sensing the quality, intensity and spatial location of painful sensations [1-4]. It is well established that SI is involved in processing innocuous tactile information, but little is known about the specific functional roles of Brodmann areas 3a, 3b, 1 and 2 within SI in processing nociceptive information. Some studies suggest involvement of areas 3b and 1 [5,6], while others implicate area 3a, [7,8], and yet others areas 1 and 2 [9]. Mapping thermal pain response with fMRI in humans have identified SI as a potentially important locus of pain processing, but, due to the lack of sufficient spatial resolution, have not resolved nociceptive somatotopy within sub-areas of SI.

A fundamental issue that remains unanswered is whether pain is represented in a topographic manner within sub-areas of SI and, if so, whether it follows the known tactile topography observed for SI. Although a somatotopy of pain has been shown in human SI [4,10-13], and stimulation of SI does interfere with pain localization [14], whether this topographic representation is specific to a sub-area within SI has not been demonstrated. A few electrophysiological studies of nociceptive somatotopy have shown localized nociceptive responses in areas 3b and 1 [5,6,15]. However, the fine topography of nociceptive representation in either 3b or 1 has not been demonstrated, leaving the question of topographic correspondence between nociceptive and tactile responses open. A clinical significance of topographic organization in pain perception is clearly demonstrated by observations that phantom limb pain may be associated with a topographic reorganization of hand or facial regions in SI [16-19]. These findings suggest that cortical reorganization in SI may lead or contribute, under certain pathological conditions, to the generation of phantom limb pain. Thus, delineating nociceptive topography is important, not only for understanding topography of normal cortical representation of pain, but also for investigating the neural mechanisms underlying pathological pain.

Another question centers on the possible differential response of sub-areas of SI to different types of pain. Most studies thus far have focused on thermal pain. However, little is known about the representation of mechanical evoked pain, despite the enormous prevalence of mechanical hyperalgesia and allodynia in chronic pain patients. Therefore, understanding the cortical representation of mechanical nociception would provide new insights on how various qualities of pain are encoded in cortex. In this study we applied mechanical nociceptive and innocuous (pressure) stimuli on individual fingerpads of humans, to measure sensations psychophysically, and anesthetized squirrel monkeys to examine whether topography of nociception is different from that of tactile touch in each of areas 3a, 3b and 1. Using this approach, we provide evidence to support the role of SI in encoding the location and intensity of mechanical nociceptive stimuli.

Methods

Surgical preparation

Four adult squirrel monkeys (*Saimiri sciureus*) were used for this study. After an initial preanesthetic dose of ketamine hydrochloride (10mg/kg), anesthesia was maintained throughout the experiment with Pentothal (sodium thiopental, 1-2 mg/kg/h, i.v.). The animal was also paralyzed with vercuronium bromide (100ug/kg/hr i.v.). Animals were artificially ventilated to maintain an end-tidal CO2 of 4%. Rectal temperature was maintained between 37-38 degrees C. Anesthetic depth was assessed continuously via implanted wire EEG electrodes, heart rate monitoring, and by regular testing for a response to toe pinch. The anesthetic state was maintained at neurosurgical anesthesia Level 2 or above (evaluated by EEG patterns). With aseptic technique, a craniotomy and durotomy were made over anterior parietal cortex. An acute imaging chamber was mounted over SI for optical imaging recording. Detailed procedures have been described previously [20-22]. All procedures were conducted

in accordance with National Institutes of Health guidelines and approved by the Vanderbilt University Animal Care and Use Committee.

Stimuli

Fingers were secured by gluing small pegs to the fingernails and fixing these pegs firmly in plasticine, leaving the glabrous surfaces available for stimulation with a mechanically controlled probe. A distal fingerpad was stimulated with two different diameter size probes attached through an armature to a force controlled torque motor. The stimuli were presented in force mode versus displacement mode, thereby reducing the possible contribution of differences in finger compliance. Probes of 2 mm (dull) and 0.2 mm (sharp) in diameter were used for delivering mechanical innocuous and nociceptive stimuli, which elicit pressure and sharp pain sensations in humans, respectively. The selection of these probe sizes was based on the results from carefully designed human psychophysical studies on mechanical pain done by Dr. Greenspan and his colleagues [23-25]. The dull and sharp probes were presented on the same digit by a stepper motor that could switch between the two probes. To determine a stimulus response function, each probe was indented with a trapezoidal waveform at a ramp rate of 1.5 N/sec and amplitudes of 0.05, 0.15, 0.30, 0.60, 0.90, 1.20 N with a duration of 3 sec. To compare the different activation patterns elicited by different size probes, stimuli perceptually rated as eliciting moderate sharp pain and moderate pressure sensations were primarily chosen for imaging experiments. Based on our psychophysical estimates (see Fig 1), these were 0.60 N for the sharp probe (0.2 mm) and 0.6 N for the dull probe (2 mm). Two stimulators were available so two digits were studied within one imaging session. Within a single imaging block, the dull probe, sharp probe and null stimulus (no stimulus, probe was off skin) conditions were presented in a randomly interleaved fashion. For electrophysiological mapping a hand-held heating probe (0.5 × 0.5 mm2 peltier device, heating ramp rate at 19 Deg C/ sec) was also used to test the response to various temperatures. Identical stimuli were used in the imaging and human psychophysical studies.

Human psychophysics

Subjects (n=6) were asked to judge in separate experimental blocks the peak magnitude of pain or pressure sensation evoked by the sharp and dull probes. Subjects were instructed to judge the magnitude of pain or pressure of each stimulus indentation by moving a computer mouse that caused a cursor to move along a visual analog scale presented on a video screen. The scale consisted of a vertical line the bottom of which was labeled as “No Sensation” and the top as “The Strongest Pain Imaginable.” Further adjectives were placed along the side of the scale: Very Strong, Strong, Moderate, Weak, and Barely Detectable, at previously specified locations [26,27]. When introduced and instructed on the use of the adjective-labeled scale (“Labeled Magnitude Scale”, LMS), subjects were given examples of strongest imaginable sensations (e.g. brightest - staring at noon into the sun; hardest - falling from a tall building onto granite; pain - dental work without analgesia; pressure - being under a pile of football players). LMS has been shown to yield psychological response functions equivalent to those produced by other magnitude estimation methods [26,27]. After the introduction, subjects were provided a few practice trials in order to feel comfortable with the paradigm. All procedures were approved by the IRB.

The back of a subject's finger was positioned at an angle of 30 degrees and fixed to a holder with double-sided tape. A drape prevented a subject from viewing his or her hand during stimulation. Prior to the beginning of an experimental session, subjects were instructed to solely rate either pain or pressure and received sample exposures to the probes. After each stimulus presentation, subjects moved the mouse along the scale to the position that corresponded to their peak sensation and then pressed the right mouse button to save that mouse position into a data file. During each task the sharp and dull probes were presented with various indentation

forces (0.15, 0.3, 0.6, 0.9, and 1.2 N) to a left distal fingerpad (D2 or D3). Mean subject magnitude estimations were obtained by presenting each stimulus 3 times in a pseudorandom order. Interstimulus intervals were 45 sec. The log of the judgment values was used to generate linear magnitude scaling functions.

Electrophysiological recording

A brief electrophysiological mapping procedure was used to locate the fingerpad region of SI (Brodmann areas 3a, 3b, and 1) prior to imaging. The central sulcus was the anatomical landmark for approximately locating areas 3b and 1. Area 3b was identified by single and multiunit properties on the basis of small receptive field size (restricted to a single finger), brisk responsiveness to light touch, and a lateral to medial topography of digits D1-D5. Area 1 was identified based on location, being found caudal to area 3b, and finding units typically with large receptive fields covering more than 1 finger [28,29]. Area 3a units usually responded to deep pressure or proprioceptive stimulation (such as joint movement), and often have large undefined receptive fields. Area 3b was typically found slightly posterior to the central sulcus (see Fig. 4E Case 1 left), and Area 3a was located anterior to Area 3b. Cortical representations of the distal fingerpads in area 3b and area 1 were segregated by the representations of the middle phalanges and palm, further identifying these cortical areas [29].

Extracellular recordings of the spike discharge activity of single neurons and local neuron populations were obtained subsequent to the optical imaging phase of the experiments. Our electrophysiological recordings mainly focused on area 3a because of our findings in the imaging experiments. Glass coated tungsten microelectrodes (Ainsworth, Northampton, UK) were inserted into superficial cortical layers and used to record unit activity from area 3a. The receptive fields (RFs) of multiple or single units were outlined through a series of indentations with a 2 mm diameter hand-held probe. Then, isolated units were classified as having a wide dynamic range (WDR) or being nociceptive specific (NS) based on their sensitivity to stimuli (mechanical or thermal) and responsiveness to graded stimulus intensities. WDR neurons characteristically show responses to stimulation intensities that range from non-noxious (< 0.3 N) to noxious levels (e.g > or = 0.3 N) while NS neurons will only respond to noxious level stimuli, review sees [30]. Conventional techniques were used to amplify, filter, and display unit activity. To store and analyze records of neuronal spike trains collected at 0.02 ms temporal resolution, we used Spike 2 hardware and software (Cambridge Electronic Design, UK).

Optical Imaging and Analysis

Image acquisition. The optical imaging procedures used were similar to those reported in previous studies [20,21,31,32]. Before imaging, an optical chamber was cemented over the craniotomy (SI area), filled with lightweight silicone oil, and sealed with a cover glass. The cortical surface was illuminated through the chamber window with 630-nm wavelength light. Images of reflectance change (intrinsic hemodynamic signals) were acquired by an Imager 3001 system (Optical Imaging Inc., Germantown, NY). Technical details and a discussion of the issues involved with intrinsic imaging have been presented previously [33-35]. Mechanical stimuli were presented in a randomly interleaved manner in blocks consisting of 10 trials per stimulus type. In a typical session, 4 to 5 blocks of trials (40-50 trials total) were collected per stimulus condition. Intrinsic signal maps were collected at 2 image frames per sec for 15 sec starting 500 ms prior to stimulus onset. Inter-stimulus intervals were between 60 and 120 sec. The stimulus probe was off the skin between stimulus presentations and during the no-stimulus condition.

Image analysis. For each stimulus condition, image trials were summed to maximize signal-to-noise ratio. To ensure that the imaged signal was not contaminated by occasional high amplitude noise, we examined images block-by-block visually to remove those that contained

excessive noise (usually due to significant blood vessel artifact). Usually all blocks were used, but occasionally a bad block was not included in subsequent analyses. We also compared images obtained by summing different blocks of trials. Presence of sporadic high amplitude noise would produce different half-trial maps, whereas consistent non-artifactual signal would produce similar maps. These methods were used to confirm that the imaged signals were consistent and repeatable and were not due to noise signals occurring in only one or a few of the trials.

Two types of image maps were generated: 'single condition' and 'two condition subtraction' maps. 'Single condition' maps were obtained by subtracting the blank (no-stimulus condition) images from those images obtained from each given stimulus (mechanical nociceptive or pressure). Single condition maps show the response magnitude at each location in the image for a particular stimulus condition. Such Blank subtractions not only measure change from baseline, but also reduce blood vessel artifact and minimize effects of uneven illumination. Dark pixels in single condition maps indicate a response to that stimulus condition greater than that of the blank condition image, gray pixels indicate a response not different from blank, and lighter pixels could indicate some level of activation less than that in blank. 'Two condition subtraction' maps were obtained by subtracting the sum of images obtained for one stimulus condition (e.g. pressure) from that obtained under another (e.g. mechanical nociceptive). Whereas single condition maps reveal the presence of a response to a particular stimulus, stimulus subtraction reveals preference for one stimulus over another. In this case, dark pixels indicate preference for one condition, light pixels a preference for the other condition, and gray pixels equal preference for both. Single condition maps provide the most reliable indication of stimulus-specific activations, but this may occur at the expense of signal-to-noise ratio (because of the contribution of noise from the blank). Difference maps yield better overall signal quality, by accentuating the preference for one condition over another, but activations common to both stimulus conditions are eliminated. Thus, single condition and subtracted maps may or may not be similar in organizational structure (e.g. see Figure 2).

Outlining activation hotspots. For each image, we delineated regions of strongest activation by using a clipping procedure. We focused on regions of strongest activation because these regions were most significantly activated by the stimulus. Images were low-pass filtered with a 4 pixel rectangular (98 × 98 μm) window and then clipped to identify pixels with strong activations. In some cases high-pass filtering was used to reduce illuminant unevenness. To identify regions of strongest activation, single condition maps were clipped at the top 15% and the subtraction maps were clipped at the top and bottom 15% of the gray pixel value distribution. Boundaries of the clipped regions were determined with 'Photoshop' software (Adobe) and overlaid with original optical maps and blood vessel maps for comparison (such as in Fig. 2B, D, F). We used identical image processing parameters for all images acquired within each case. Although the activation boundary shifted slightly with different high-pass, low-pass, and thresholding criteria, our conclusions were not dependent on slight differences in such criteria. In this paper, we present with the original unprocessed image these outlines as a guide to the reader for the qualitative comparison of maps obtained within each imaging session.

Results

Psychophysical evaluation on sensations elicited by indentation with different size probes

To determine the range of stimulus parameters, we conducted human psychophysical studies on 6 subjects to obtain estimates of perceived pain and pressure magnitudes for the 0.2 mm (sharp) and 2 mm (dull) diameter probes for the distal fingerpads. Figure 1 illustrates the peak magnitude of pain (A) and pressure (B) sensation as a function of indentation force. Graphing the data on a log-log scale linearized the psychophysical function. During the pain rating

session (A), only indentations with 0.2 mm diameter probe were rated as painful. No painful sensation was evoked by indentation with the 2 mm diameter probe within the force range tested (0.05 to 1.2 Newton, each symbol indicate ratings from an individual subject). The threshold for a judgment of weak pain for these 6 subjects occurred with an indentation force of about 0.3 N (dotted vertical line); whereas, 0.6 N and 0.9 N indentations with 0.2 mm diameter probe evoked moderate and strong sharp pain sensations, respectively. Subjects anecdotally reported that at 0.9 N a deep proprioceptive pain accompanied the sharp stinging pain.

In contrast, when the same subjects rated the pressure sensation (Fig. 1B), the magnitudes of pressure sensation evoked by 0.2 and 2 mm probe were comparable as observed by the similarity of the fitted slopes for the 0.2 mm probe (black line) and the 2 mm probe (gray line). Moderate and strong pressure sensations were produced with the 2 mm probe at 0.6 N and 0.9 N indentations, respectively. Based on these results, we determined that 0.3, 0.6, or 0.9 N indentations with the 0.2 mm probe produced perceptually comparable magnitudes of weak, moderate, and strong pain or pressure sensations as the 2 mm diameter probe. Since humans and monkeys are reported to have comparable pain thresholds[36-39], in this study on monkeys, we used the same stimuli that were rated by humans as weak, moderate, or strong. We will refer to 0.3 N, 0.6 N, 0.9 N indentation of 0.2 mm probe as our weak, moderate, and strong sharp nociceptive stimuli, and 0.3 N, 0.6 N, 0.9 N indentation of 2 mm diameter probe as our weak, moderate and strong pressure stimuli.

Electrophysiology

Prior to imaging, we conducted brief electrophysiological sampling of neural response preferences and receptive field sizes in areas 3a, 3b, and 1. This helped define the imaging field of view and to estimate areal borders (cf. Figures 5 and 7). Typically, we examined responsiveness to tactile stimulation (light brush, tapping, dull probe), proprioceptive stimulation (passive finger movement, tendon stimulation), and noxious stimulation (pinch, squeeze, sharp probe indentation, heating provided by a peltier device). One example of a multi-unit recording that responded to both dull probe and sharp probe stimuli is shown in Figure 2. Fig. 2A illustrates the recording site (white circle) in area 3a that was in a location that exhibited a response to sharp probe stimulation of D5 during optical imaging (see Figure 3 below). The mapped receptive field was large, occupying the entire glabrous surfaces of fingers D4 and D5. Fig. 2B shows the PSTH (post-stimulus time histogram) of this unit's response (sum of 20 trials) to indentation of the dull probe (B) and sharp probe (C). Although this unit exhibited responsiveness to both dull and sharp probe stimuli, the response to a moderate nociceptive stimulus (0.6 N sharp probe indentation) evoked the most robust and sustained response (Fig. 2C, right graph). This neuron is typical of what has been previously classified as wide dynamic range (WDR) nociceptive neurons[30, 40]. Thus far, we have recorded six neurons of this type, all of which were located in area 3a. These recordings suggested the presence of neural responses to mechanical nociceptive stimulation. We then mapped such responses with optical imaging methods.

Temporal profiles of optical response in SI to nociceptive stimuli

We collected 8 imaging data sets from 4 squirrel monkeys. Images from 4 data sets are illustrated in the paper. Data from 7 data sets are summarized in Figure 8.

We evaluated the temporal profile of the optical signal to nociceptive stimulation in the anesthetized monkeys. In Fig. 3A-C, we illustrate the temporal development of optical imaging maps in response to 0.6 N sharp (A) and dull probe (B) stimulations of D3. Areal borders are indicated by dotted lines in the last panel of 3C. In the nociceptive condition (A, 0.6 N indentation of sharp probe for 3 sec), area 3b activations (indicated by the dark patch in the

center of field of view) began around 1.5 sec after stimulus onset, peaked around 3 sec, and then remained active till the end of the 12 sec imaging period. The onset latencies in areas 3a and 1 occurred later (dark patches on both left and right 1/3 column as indicated by arrows in 5 sec image in Fig. 3A). In the innocuous condition (B, 0.6N indentation of dull probe for 3 sec), activation began around 1.5 sec, but declined immediately after 2.5 sec. Baseline is shown by the no stimulus condition in Fig 3C (no probe contact). The timecourses of the optical signal taken from three regions of interest (locations shown by black boxes on the last panel of 3C) in areas 3a, 3b and 1 are plotted in Fig 3D-F, where gray and black curves plot change in light reflectance (dR/R %) in response to 0.6 N sharp and dull probe (3 sec indentation, gray bar in Fig. 6D) and in the no stimulus condition, respectively. In general, optical signal evoked by brief sharp probe indentation lasts longer than responses to innocuous stimuli. This is consistent with the thermal nociceptive response in area 3a [8] and contrasts to the typical tactile response timecourse [21]. The sustained timecourse of nociceptive response could reflect the sustained and slowly adapting neural activity previously reported in SI cortex [5, 6, 15, 30].

Topography of nociceptive response in areas 3a, 3b and 1

To examine whether nociceptive responses are represented topographically in SI, in two animals we mapped the activation of pairs of individual fingerpads to the sharp probe stimulus (0.6 N). In one animal (case 1), we presented mechanical nociceptive stimulation to D5 (Fig. 4A, red outlines in 4B) and to D3 (Fig. 4C, blue outlines in 4D). These evoked 0.5-1.5 mm sized activations in areas 3a, 3b and 1 (borders between areas shown in 4E). Superimposition of these activations on the blood vessel map (Fig. 4E) reveals a clear somatotopy in both areas 3b and 1. D5 activations (red) were located more medially than D3 activations (blue), consistent with our electrophysiological map (yellow and green dots in areas 3b and 1, respectively) and with previous studies [20, 21, 29, 41, 42]. In area 3a, greater overlap between D5 and D3 activation was observed, but appropriate somatotopy was retained. This is comparable to the existing literature suggesting that neurons in area 3a tend to have large undefined receptive fields [43, 44]. In the second animal (Case 2), somatotopically organized activations to nociceptive stimulation of D4 (Fig. 4A, red outlines in B) and D3 (Fig. 4C, blue outlines in D) were observed in both areas 3b and 1 (superimposed map shown in Fig. 4E, area 3a was not in the field of view). Again, appropriate topographic organization was present in both areas 3b and 1, consistent with electrophysiological recordings. Taken together, these data demonstrate that sharp probe induced nociceptive response is somatotopically represented in areas 3a, 3b and 1.

Activation patterns within SI during nociceptive versus pressure stimulation

To determine whether areas 3a, 3b, or 1 are differentially activated by mechanical innocuous and nociceptive inputs, 0.6 N sharp (moderate nociceptive, Fig 5A-B) and 0.6 N dull (moderate pressure, Fig 5C-D) were presented on the distal fingerpads (digit D3 as shown in Fig. 5). As shown in Fig 5A (areas 3a, 3b and 1, borders indicated by red dotted lines), in response to presentation of the sharp probe on D3, three spatially distinct activations (activations outlined in blue in Fig 5B) were observed in single condition maps, one in area 3a, 3b, and area 1. With the dull probe, two focal activations were obtained, one in area 3b and area 1 (Fig. 5C, red outlines in 5D); this tactile response pattern is consistent with our previous studies [20,21, 45].

Based on our psychophysics, we determined that the sharp and dull probes when presented with equal force produce comparable judgments of pressure. Therefore, we reasoned that, since the tactile component is comparable for both sharp and dull probes at equal indentation forces, one could remove (at least in part) the tactile component of the sharp probe response by subtracting the dull probe response from the sharp probe response. Thus, this subtraction is intended to reveal the preferential nociceptive response. In the sharp minus dull subtraction

maps shown in Figure 5E and F, the dark pixels indicate preference for the sharp probe, i.e. preference for the nociceptive stimulus. These dark pixels were found primarily in areas 3a and 1 (green outlines in F); little preference for the sharp probe stimulus was observed in area 3b.

Encoding of nociceptive intensity in SI

One indicator that a cortical area may be involved in nociception is a correlation of response magnitude to nociceptive stimulus intensity. Figure 6 shows the images acquired in response to four stimulus intensities: 0.15 N sharp probe (not nociceptive, Fig. 6A and 6B), 0.3 N sharp probe (weakly nociceptive, Fig. 6C and 6D), 0.6N sharp probe (moderately nociceptive, Fig. 6E and 6F), and no stimulus condition (6G). These images illustrate two points. First, in areas 3b and 1, activation sizes increased with stimulus intensity (compare 6B, 6D and 6F) when the sharp probe intensity increased from not nociceptive to very weak and moderately nociceptive. Second, the higher stimulus intensity additionally recruited area 3a (indicated by the red arrow in Fig. 6E). In the no stimulus condition (Fig. 6G), a flat map lacking areas of activation was observed.

To examine the magnitude of response, we selected regions of interest (indicated by the red boxes in Fig. 6H, same image as 6F) at each center of activation in areas 3a, 3b and 1, and measured the amplitudes of the optical signal. All three areas showed a graded response with stimulus intensity as sharp probe indentation force increased from 0.15 N to 0.3 N to 0.6 N and were of greater signal amplitude than the no stimulus condition (Fig. 6I), suggesting that all three areas may be involved in mechanical nociceptive intensity coding.

Graded responses in areas 3b and 1 to increasing intensities of innocuous stimulation

Given the simultaneous recruitment of activity from both innocuous tactile and nociceptive neurons during mechanical nociceptive stimulation, one way to assess the nociceptive contribution would be comparing the stimulus-response functions between innocuous tactile and nociceptive stimulus conditions. Therefore, in an effort to dissociate the pressure component from the nociceptive component of the sharp probe stimulus, we wanted to quantify the stimulus response functions for both sharp and dull probes. Thus we examined the signal response to increasing pressure intensity with the dull probe. Shown in Fig. 7 are activations to the dull probe on digit D3: to 0.6 N (A: moderate pressure, red outlines in B) and 0.9 N (C: strong pressure, red outlines in D). The no stimulus condition is shown in E. Consistent with our previous studies [45,46], tactile stimulation with the dull probe evoked only activations in areas 3b and 1, but not in area 3a (areal borders indicated by dotted lines in F). Slightly enlarged activations (comparing left red outlined regions in D and B) were evident when stimulus intensity increased from 0.6 to 0.9 N. In area 1, such a change was not obvious in terms of spatial extent. Although spatial differences in activation with different intensities were minimal, when the amplitudes of optical signal were measured in each area (signal measurements were taken from regions indicated by red boxes in Fig. 7F), we observed greater signal amplitudes with the 0.9 N pressure stimuli (red columns) than the 0.6 N pressure (green columns, Fig. 7G) in both area 3b (middle column group) and area 1 (right column group). Pressure responses were greater than the no stimulus condition (gray column) in both areas 3b and 1. The response in area 3b is consistent with our previous observations [20,45,46]. In comparison with Fig. 6I (nociceptive responses evoked by sharp probe), the clearest difference in the activation pattern was in area 3a (summary of 15 trials), where only the sharp probe was found to activate area 3a. Thus, at least some of the response obtained with the nociceptive probe (especially that in area 3a, Figure 6) is not due solely to the pressure component.

Comparison of signal amplitudes to nociceptive and innocuous mechanical stimuli

Across cases (n=7), we observed differential stimulus response function curves in sharp and dull probe conditions (Figure 8). There are several characteristics worth noting. First of all, in sharp probe conditions, stimulus intensity-response amplitude curves changed dramatically at the intensity of 0.3N (black arrow in Fig. 8A) in areas 3a, 3b and 1. At intensities of 0.6N and 0.9N (>0.3N in Fig. 8C), at which moderate to strong pain sensations were evoked in human subjects (r.f. Fig 1), signal amplitudes were significantly greater ($p<0.05$, student t-test) than that in no stimulus (blank) conditions in all three areas of 3a, 3b and 1 (comparing the black with the white columns in Fig. 8C). This finding suggests that areas 3a, 3b and 1 responded significantly to mechanical nociceptive stimuli. When we compared the signal amplitudes in response to nociceptive (Fig. 8C, 0.6N and 0.9N; black columns; >0.3N) versus innocuous (gray columns; 0.05, 0.15N; < 0.3N) sharp probe indentation, stronger signal was observed for all areas, but only for area 3b was the difference statistically significant ($p<0.05$, middle column groups in Fig. 8C). This data suggests that statistically, only area 3b responded in a stimulus-intensity dependent manner for the entire innocuous to nociceptive intensity range tested. In contrast, in dull probe conditions, generally linear increasing curves were present in areas 3b (solid line in Fig. 8B) and 1 (dashed line) in the 0.15N to 0.9N intensity range, but a pretty flat response from 0.3N to 0.9N was found for area 3a (dotted line). For the dull probe, when we divided the responses to low (0.15 and 0.3N, </= 0.3, black columns in Fig. 8D) and high (0.6N and 0.9N, >0.3N, gray columns) intensity groups, significant signal amplitude differences were observed in areas 3b (middle column group) and 1 (right column group). Similarly, signal amplitude at higher intensity was significantly different than the no stimulus (blank condition, white columns) in areas 3b and 1. Importantly, in area 3a, no significant signal differences were observed between groups (left column group in Fig. 8D). In sum, significant differences were observed for the dramatic response increases in areas 3a, 3b and 1 at nociceptive intensities of the sharp probe, and no significant signal changes were found in area 3a with the dull probe. Finally, one thing to note is that generally responses evoked by sharp probe were greater than that evoked by dull probe (comparing left panels of A C with right panels of B&D) even though perceptually they elicit comparable magnitudes of sensation. This difference could contribute to the encoding of nociceptive component of the stimulus.

Discussion

Summary

In this study, we used optical imaging of intrinsic signals (OIS) to examine the organization of mechanical nociceptive response within primary somatosensory cortex (SI) of anesthetized squirrel monkeys. We compared cortical responses to the indentation of sharp (0.2 mm) and dull (2 mm) probes on individual distal finger pads. Stimulus intensities presented were those that elicited nociceptive (sharp) and pressure (dull) sensations rated as weak, moderate, or strong in humans. We found that mechanical nociceptive activation of individual digits was organized somatotopically within areas 3a, 3b and 1, and co-localized with activations to pressure responses in areas 3b and 1. Although all three areas exhibited response to mechanical nociceptive stimulation, innocuous pressure generated activations in areas 3b and 1 but not in area 3a. Only area 3b showed significant differences in response between nociceptive and innocuous stimuli. Intensity dependent responses to nociceptive stimuli were observed in all areas, but only in areas 3b and 1 showed intensity dependent responses to pressure, consistent with our previous reports [21,46]. These findings demonstrate that all three areas (3a, 3b and 1) are involved in the processing of inputs evoked by sharp probe indentation, but only area 3a responded more selectively to the nociceptive components.

Area-specific representation of mechanically nociceptive inputs within primary somatosensory cortex

Even though mechanical hyperalgesia and allodynia are a clinically significant complaint, only a few imaging studies have been performed with mechanically evoked painful stimuli [48-51]. In comparison with thermal painful stimuli, where the sensation of temperature is muted by the sensation of pain, the sensations of pressure and sharp pain are both perceived when the sharp probe was indented, as indicated previously [23,47] and by our own human psychophysical studies (Fig. 1). Thus, one of the challenges posed in studying mechanically evoked pain is dissociating the tactile and painful components inherent in the stimulus. This dissociation is critical in interpreting the modality specificity of the activation as revealed in imaging studies.

In this study, we have approached these difficulties in a few different ways. The first was to identify pressure and nociceptive stimuli that induce comparable sensation magnitudes of pressure and pain in humans. One assumption is that monkeys and humans have comparable perceptual sensitivities and thresholds. This is supported by previous studies. For example, monkeys and humans exhibit similar sensitivities to small temperature changes that are above thermal pain thresholds [36-39]. Additionally, peripheral nociceptive fibers and neurons in primate SI primate respond to thermal stimulation in the range that humans report as painful [36,38,39]. Although there are no studies comparing mechanical nociceptive perception in humans and monkeys, there is evidence to support that noxious mechanical stimuli, which was perceived as painful, elicited similar nociceptive responses in human thalamus [48] as in the awake monkey thalamus [49]. Therefore, it is reasonable to assume that painful mechanical stimuli for humans would be also painful in monkeys and that the monkeys and humans have similar thresholds to mechanical pain.

Secondly, we tried to remove, at least in part, the tactile component of the mechanical nociceptive stimulus. Towards this end, we subtracted the pressure (purely tactile) responses from mechanical nociceptive (tactile plus nociceptive) responses. This revealed that the greatest differential response to nociceptive versus pressure stimuli occurred in area 3a. Together, these data support a preferential role of area 3a in the cortical encoding of mechanical nociception.

Although studies in humans suggest different activation loci within SI for thermal pain and touch [9], limitations of the spatial specificity of those mapping techniques limits the ability to map these activations to specific Brodmann areas. By using optical imaging (which provides a spatial resolution of 50-100 micron), we demonstrate that mechanical nociceptive and innocuous pressure stimuli evoke different inter-areal activation patterns: areas 3a, 3b and 1 are activated during mechanical nociceptive stimulation, while only areas 3b and 1 are activated during innocuous tactile stimulation. Therefore, mechanical nociception is represented in multi-areal activation patterns within SI. Area 3a more selectively responded to mechanical nociceptive information.

Within areas 3b and 1 nociceptive and tactile responses were co-localized. If there were nociceptive specific representations, one would expect to see separate nociceptive and tactile responsive clusters in subtraction maps. When we subtracted pressure response from the nociceptive response, a common imaging processing procedure used to remove or reduce common signal and emphasize differential responses, activations in area 3a and to some degree in area 1 remained while most of the focal activation in area 3b was diminished. This observation suggested regions of clustered activation to nociceptive stimulation were found in area 3a, and in area 1 to a lesser extent, but not in area 3b. In other words, there were inter-areal activation differences in the responses to the sharp and dull probes. Inter-areal activation

pattern differences to nociceptive versus innocuous stimuli have also been suggested in human studies [50-52].

We speculate that area 3b could play a larger role than areas 1 and 3a in encoding the pressure component of the nociceptive stimulus while areas 3a and 1 may play a greater role in processing nociceptive information. These conclusions are in line with previous electrophysiology studies. It has been shown that areas 3b and 1 are primary tactile processing areas since the majority of their neurons respond to inputs from low threshold mechanoreceptors, review see [53,54]. With respect to nociceptive processing, only a relatively small number of nociceptive neurons (both WDR and NS neurons) were identified among low threshold tactile neurons in areas 3b and 1 [5,6], as well as in area 3a [8]. Adding to those previous studies, we have demonstrated that among the activated areas, area 3a exhibited greatest preferential response to a mechanical nociceptive stimulus. Together with the isolation of mechanical nociceptive responsive neurons in those activated regions, our study has extended the previous reports on the involvement of area 3a in the processing of heat nociceptive inputs [7,8], by supporting a general role of area 3a in the processing of nociceptive inputs. However, because we did not test responses to other types of stimuli that can active area 3a (e.g. tendon vibration or finger movement, [43,44]) in this experiment, we cannot predicate the relationship of nociceptive processing with other known functions of area 3a as suggested by single unit electrophysiology. In summary, we hypothesized that mechanical pain information is preferentially represented in areas 3a while pressure information is encoded in areas 3b and 1. Given the nature of imaging studies, whose signal derives from populations of neurons [33,55], intensive single unit recordings are needed to characterize the neuronal activities of both tactile and nociceptive units to understand the single neuron basis underlying the activations measured with optical signal.

Topography of mechanical pain in SI

In our study, we focused on a small region of the somatosensory cortex representing only the distal fingerpads. Mapping the distal fingerpad region is important, as the distal fingerpads have the largest somatosensory cortical representation. Our optical imaging data revealed orderly focal (1.0-1.5 mm) representations to nociceptive indentation of individual distal fingerpads in areas 3a, 3b and 1, that is consistent with other investigations which have demonstrated a gross somatotopic organization of pain in SI, such as that between the hand and foot in SI [10,12,56] and also advances our understanding of nociceptive topography to-specific areas (i.e. area 3a, 3b, 1) within SI. Thus, within SI, the representation of nociceptive inputs exhibits a topography, which is closely associated with and overlaps the topography for tactile processing. Although topographically aligned with tactile representation, area 3a exhibits greater differential response to nociceptive stimulation than 3b and 1. These findings help to further localize cortical sites of nociceptive processing in the somatosensory system.

Conclusion

Our study has demonstrated that mechanical nociceptive inputs were processing in areas of 3a, 3b and 1 whereas innocuous tactile inputs were mainly represented in areas 3b and 1. Within areas of 3b and 1, nociceptive responses were co-localized with tactile responses and were somatotopically organized. A cruder somatotopy for nociceptive stimuli was present in areas 3a. Quantitative measurements of cortical responses to various intensities of mechanical nociceptive and tactile stimuli suggested a trend for nociceptive intensity coding in areas 3a, 3b and 1. We hypothesize that nociception is represented in SI where specific activation patterns within SI sub-areas code the location and modality of a nociceptive stimulus.

Acknowledgements

We thank F.L. Healy for excellent technical assistance. This work was supported by grants from NIH NS044375 (AWR), NIH DE016606 (LMC) and the Packard (AWR) and Brown-Coxe Foundations (LMC).

References

1. Apkarian AV, Bushnell MC, Treede RD, Zubieta JK. Human brain mechanisms of pain perception and regulation in health and disease. Eur J Pain 2005;9:463. [PubMed: 15979027]
2. Bushnell MC, Duncan GH, Hofbauer RK, Ha B, Chen JI, Carrier B. Pain perception: is there a role for primary somatosensory cortex? Proc Natl Acad Sci U S A 1999;96:7705. [PubMed: 10393884]
3. Duncan GH, Albanese MC. Is there a role for the parietal lobes in the perception of pain? Adv Neurol 2003;93:69. [PubMed: 12894402]
4. Strigo IA, Duncan GH, Boivin M, Bushnell MC. Differentiation of visceral and cutaneous pain in the human brain. J Neurophysiol 2003;89:3294. [PubMed: 12611986]
5. Kenshalo DR Jr, Isensee O. Responses of primate SI cortical neurons to noxious stimuli. J Neurophysiol 1983;50:1479. [PubMed: 6663338]
6. Kenshalo DR, Iwata K, Sholas M, Thomas DA. Response properties and organization of nociceptive neurons in area 1 of monkey primary somatosensory cortex. J Neurophysiol 2000;84:719. [PubMed: 10938299]
7. Tommerdahl M, Delemos KA, Favorov OV, Metz CB, Vierck CJ Jr, Whitsel BL. Response of anterior parietal cortex to different modes of same-site skin stimulation. J Neurophysiol 1998;80:3272. [PubMed: 9862921]
8. Tommerdahl M, Delemos KA, Vierck CJ Jr, Favorov OV, Whitsel BL. Anterior parietal cortical response to tactile and skin-heating stimuli applied to the same skin site. J Neurophysiol 1996;75:2662. [PubMed: 8793772]
9. Valeriani M, Barba C, Le Pera D, Restuccia D, Colicchio G, Tonali P, Gagliardo O, Treede RD. Different neuronal contribution to N20 somatosensory evoked potential and to CO2 laser evoked potentials: an intracerebral recording study. Clin Neurophysiol 2004;115:211. [PubMed: 14706490]
10. Andersson JL, Lilja A, Hartvig P, Langstrom B, Gordh T, Handwerker H, Torebjork E. Somatotopic organization along the central sulcus, for pain localization in humans, as revealed by positron emission tomography. Exp Brain Res 1997;117:192. [PubMed: 9419066]
11. DaSilva AF, Becerra L, Makris N, Strassman AM, Gonzalez RG, Geatrakis N, Borsook D. Somatotopic activation in the human trigeminal pain pathway. J Neurosci 2002;22:8183. [PubMed: 12223572]
12. Tarkka IM, Treede RD. Equivalent electrical source analysis of pain-related somatosensory evoked potentials elicited by a CO2 laser. J Clin Neurophysiol 1993;10:513. [PubMed: 8308146]
13. Vogel H, Port JD, Lenz FA, Solaiyappan M, Krauss G, Treede RD. Dipole source analysis of laser-evoked subdural potentials recorded from parasylvian cortex in humans. J Neurophysiol 2003;89:3051. [PubMed: 12783950]
14. Porro CA, Martinig M, Facchin P, Maieron M, Jones AK, Fadiga L. Parietal cortex involvement in the localization of tactile and noxious mechanical stimuli: a transcranial magnetic stimulation study. Behav Brain Res 2007;178:183. [PubMed: 17239452]
15. Kenshalo, DR.; Willis, WD. The role of cerebral cortex in pain sensation. New York: Plenum Press; 1991.
16. Birbaumer N, Lutzenberger W, Montoya P, Larbig W, Unertl K, Topfner S, Grodd W, Taub E, Flor H. Effects of regional anesthesia on phantom limb pain are mirrored in changes in cortical reorganization. J Neurosci 1997;17:5503. [PubMed: 9204932]
17. Flor H, Elbert T, Knecht S, Wienbruch C, Pantev C, Birbaumer N, Larbig W, Taub E. Phantom-limb pain as a perceptual correlate of cortical reorganization following arm amputation. Nature 1995;375:482. [PubMed: 7777055]
18. Pleger B, Tegenthoff M, Schwenkreis P, Janssen F, Ragert P, Dinse HR, Volker B, Zenz M, Maier C. Mean sustained pain levels are linked to hemispherical side-to-side differences of primary

somatosensory cortex in the complex regional pain syndrome I. Exp Brain Res 2004;155:115. [PubMed: 15064892]

19. Tinazzi M, Valeriani M, Moretto G, Rosso T, Nicolato A, Fiaschi A, Aglioti SM. Plastic interactions between hand and face cortical representations in patients with trigeminal neuralgia: a somatosensory-evoked potentials study. Neuroscience 2004;127:769. [PubMed: 15283973]
20. Chen LM, Friedman RM, Ramsden BM, LaMotte RH, Roe AW. Fine-scale organization of SI (area 3b) in the squirrel monkey revealed with intrinsic optical imaging. J Neurophysiol 2001;86:3011. [PubMed: 11731557]
21. Chen LM, Friedman RM, Roe AW. Optical imaging of a tactile illusion in area 3b of the primary somatosensory cortex. Science 2003;302:881. [PubMed: 14500850]
22. Friedman RM, Chen LM, Roe AW. Modality maps within primate somatosensory cortex. Proc Natl Acad Sci U S A 2004;101:12724. [PubMed: 15308779]
23. Greenspan JD, McGillis SL. Stimulus features relevant to the perception of sharpness and mechanically evoked cutaneous pain. Somatosens Mot Res 1991;8:137. [PubMed: 1887724]
24. Greenspan JD, McGillis SL. Thresholds for the perception of pressure, sharpness, and mechanically evoked cutaneous pain: effects of laterality and repeated testing. Somatosens Mot Res 1994;11:311. [PubMed: 7778408]
25. Sarlani E, Greenspan JD. Gender differences in temporal summation of mechanically evoked pain. Pain 2002;97:163. [PubMed: 12031789]
26. Green B, Shaffer G, Gilmore M. Derivation and evalulation of a semantic scale of oral sensation magnitude with apparent ratio properties. Chem Senses 1993;18:405.
27. Green BG, Dalton P, Cowart B, Shaffer G, Rankin K, Higgins J. Evaluating the 'Labeled Magnitude Scale' for measuring sensations of taste and smell. Chem Senses 1996;21:323. [PubMed: 8670711]
28. Iwamura Y, Tanaka M, Sakamoto M, Hikosaka O. Rostrocaudal gradients in the neuronal receptive field complexity in the finger region of the alert monkey's postcentral gyrus. Exp Brain Res 1993;92:360. [PubMed: 8454001]
29. Sur M, Nelson RJ, Kaas JH. Representations of the body surface in cortical areas 3b and 1 of squirrel monkeys: comparisons with other primates. J Comp Neurol 1982;211:177. [PubMed: 7174889]
30. Willis, WDJ. The pain system: The neural basis of nociceptive transmission in the mammalian nervous system. New York: Karger; 1985.
31. Roe AW, Ts'o DY. Specificity of color connectivity between primate V1 and V2. J Neurophysiol 1999;82:2719. [PubMed: 10561440]
32. Roe AW, Ts'o DY. Visual topography in primate V2: multiple representation across functional stripes. J Neurosci 1995;15:3689. [PubMed: 7751939]
33. Bonhoeffer, T.; Grinvald, A. Optical imaging based on intrinsic signals: The methodology. London: Academic Press; 1996.
34. Grinvald A, Frostig RD, Lieke E, Hildesheim R. Optical imaging of neuronal activity. Physiol Rev 1988;68:1285. [PubMed: 3054949]
35. Ts'o DY, Frostig RD, Lieke EE, Grinvald A. Functional organization of primate visual cortex revealed by high resolution optical imaging. Science 1990;249:417. [PubMed: 2165630]
36. Bushnell MC, Taylor MB, Duncan GH, Dubner R. Discrimination of innocuous and noxious thermal stimuli applied to the face in human and monkey. Somatosens Res 1983;1:119. [PubMed: 6679916]
37. Chudler EH, Anton F, Dubner R, Kenshalo DR Jr. Responses of nociceptive SI neurons in monkeys and pain sensation in humans elicited by noxious thermal stimulation: effect of interstimulus interval. J Neurophysiol 1990;63:559. [PubMed: 2329361]
38. LaMotte RH, Thalhammer JG, Robinson CJ. Peripheral neural correlates of magnitude of cutaneous pain and hyperalgesia: a comparison of neural events in monkey with sensory judgments in human. J Neurophysiol 1983;50:1. [PubMed: 6875640]
39. LaMotte RH, Torebjork HE, Robinson CJ, Thalhammer JG. Time-intensity profiles of cutaneous pain in normal and hyperalgesic skin: a comparison with C-fiber nociceptor activities in monkey and human. J Neurophysiol 1984;51:1434. [PubMed: 6737035]
40. Willis WD Jr. Pain pathways in the primate. Prog Clin Biol Res 1985;176:117. [PubMed: 3923492]

41. Pons TP, Garraghty PE, Cusick CG, Kaas JH. A sequential representation of the occiput, arm, forearm and hand across the rostrocaudal dimension of areas 1, 2 and 5 in macaque monkeys. Brain Res 1985;335:350. [PubMed: 4005565]

42. Pons TP, Wall JT, Garraghty PE, Cusick CG, Kaas JH. Consistent features of the representation of the hand in area 3b of macaque monkeys. Somatosens Res 1987;4:309. [PubMed: 3589287]

43. Huffman KJ, Krubitzer L. Area 3a: topographic organization and cortical connections in marmoset monkeys. Cereb Cortex 2001;11:849. [PubMed: 11532890]

44. Krubitzer L, Huffman KJ, Disbrow E, Recanzone G. Organization of area 3a in macaque monkeys: contributions to the cortical phenotype. J Comp Neurol 2004;471:97. [PubMed: 14983479]

45. Chen LM, Friedman RM, Roe AW. Optical imaging of SI topography in anesthetized and awake squirrel monkeys. J Neurosci 2005;25:7648. [PubMed: 16107651]

46. Friedman RM, Chen LM, Roe AW. Responses of Area 1 in Anesthesized Squirrel Monkeys to Single and Dual Site Stimulation of the Digits. J Neurophysiol. 2008under revision

47. Greenspan JD, Thomadaki M, McGillis SL. Spatial summation of perceived pressure, sharpness and mechanically evoked cutaneous pain. Somatosens Mot Res 1997;14:107. [PubMed: 9399411]

48. Lenz FA, Gracely RH, Rowland LH, Dougherty PM. A population of cells in the human thalamic principal sensory nucleus respond to painful mechanical stimuli. Neurosci Lett 1994;180:46. [PubMed: 7877759]

49. Casey KL, Morrow TJ. Ventral posterior thalamic neurons differentially responsive to noxious stimulation of the awake monkey. Science 1983;221:675. [PubMed: 6867738]

50. Lui F, Duzzi D, Corradini M, Serafini M, Baraldi P, Porro CA. Touch or pain? Spatio-temporal patterns of cortical fMRI activity following brief mechanical stimuli. Pain. 2008

51. Ploner M, Schmitz F, Freund HJ, Schnitzler A. Differential organization of touch and pain in human primary somatosensory cortex. J Neurophysiol 2000;83:1770. [PubMed: 10712498]

52. Timmermann L, Ploner M, Haucke K, Schmitz F, Baltissen R, Schnitzler A. Differential coding of pain intensity in the human primary and secondary somatosensory cortex. J Neurophysiol 2001;86:1499. [PubMed: 11535693]

53. Kaas JH. Evolution of somatosensory and motor cortex in primates. Anat Rec A Discov Mol Cell Evol Biol 2004;281:1148. [PubMed: 15470673]

54. Kaas JH. The functional organization of somatosensory cortex in primates. Ann Anat 1993;175:509. [PubMed: 8297039]

55. Davis KD. Neurophysiological and anatomical considerations in functional imaging of pain. Pain 2003;105:1. [PubMed: 14499413]

56. Xu X, Fukuyama H, Yazawa S, Mima T, Hanakawa T, Magata Y, Kanda M, Fujiwara N, Shindo K, Nagamine T, Shibasaki H. Functional localization of pain perception in the human brain studied by PET. Neuroreport 1997;8:555. [PubMed: 9080447]

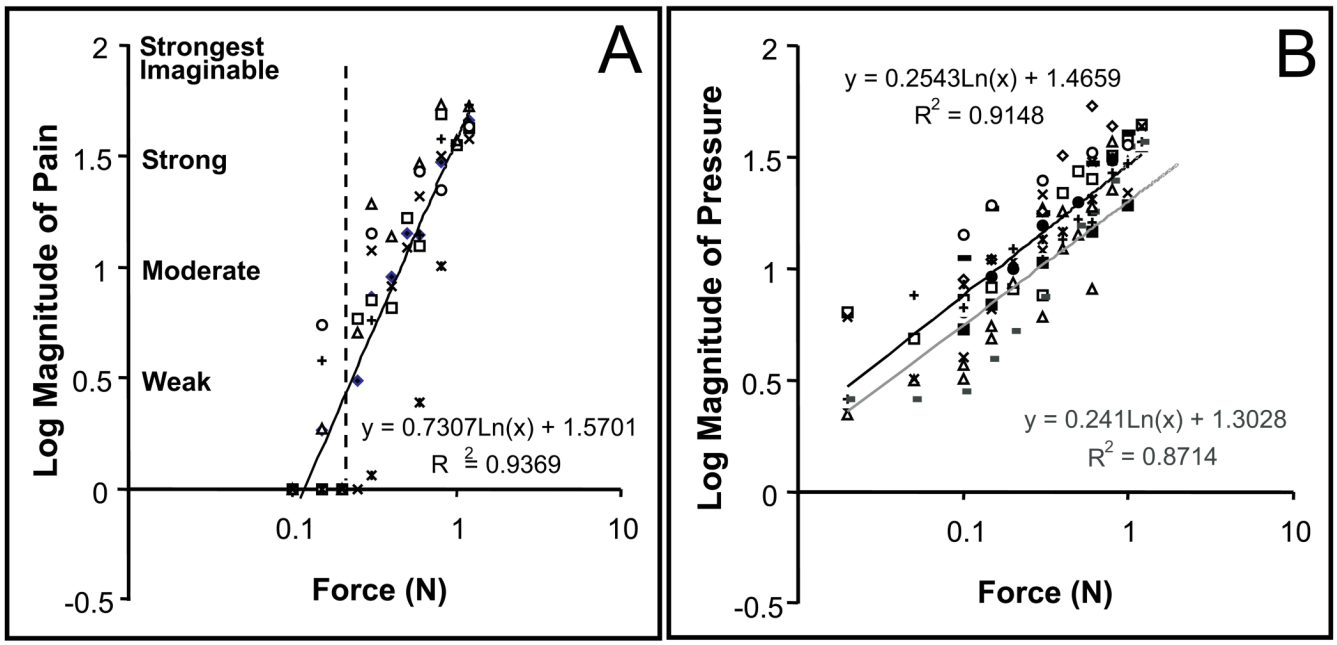

Figure 1.

Estimations of pain and pressure magnitudes for the 2 different diameter probes. A) Magnitude estimations of pain. Only indentations of 0.2 mm diameter probe with force of 0.3 N or above were judged as painful. Average threshold to elicit a weak pain was about 0.3 N (dashed line). B) Magnitude estimations of pressure. The magnitude estimations of pressure overlapped for the 2 probes: 0.2 mm probe, line of black. 2 mm probe, line of gray. The fitted regression equations are shown on the right. Each symbol (triangle, square, or circle etc) represents the average rating from an individual subject. These observations are consistent with a previous report [23].

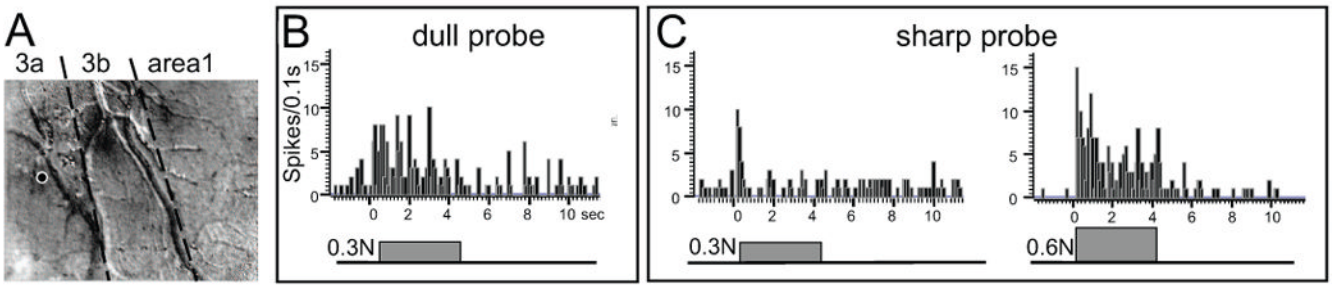

Figure 2.

An area 3a wide dynamic range unit studied with the 2 and 0.2 mm probes. A) Electrode location centered in area 3a in the region activated by the 0.2 mm probe, as shown for 0.9 N indentation. Dark areas indicate activation. B) PSTH in response to the 2 mm diameter probe indented with 0.3 N. C) PSTH in response to the 0.2 mm diameter probe indented with 0.3 N. and 0.6 N. Lines beneath PSTHs indicate duration of stimulus. Sum of 20 trials. Note that the unit responded to both low pressure and moderate nociceptive stimulation.

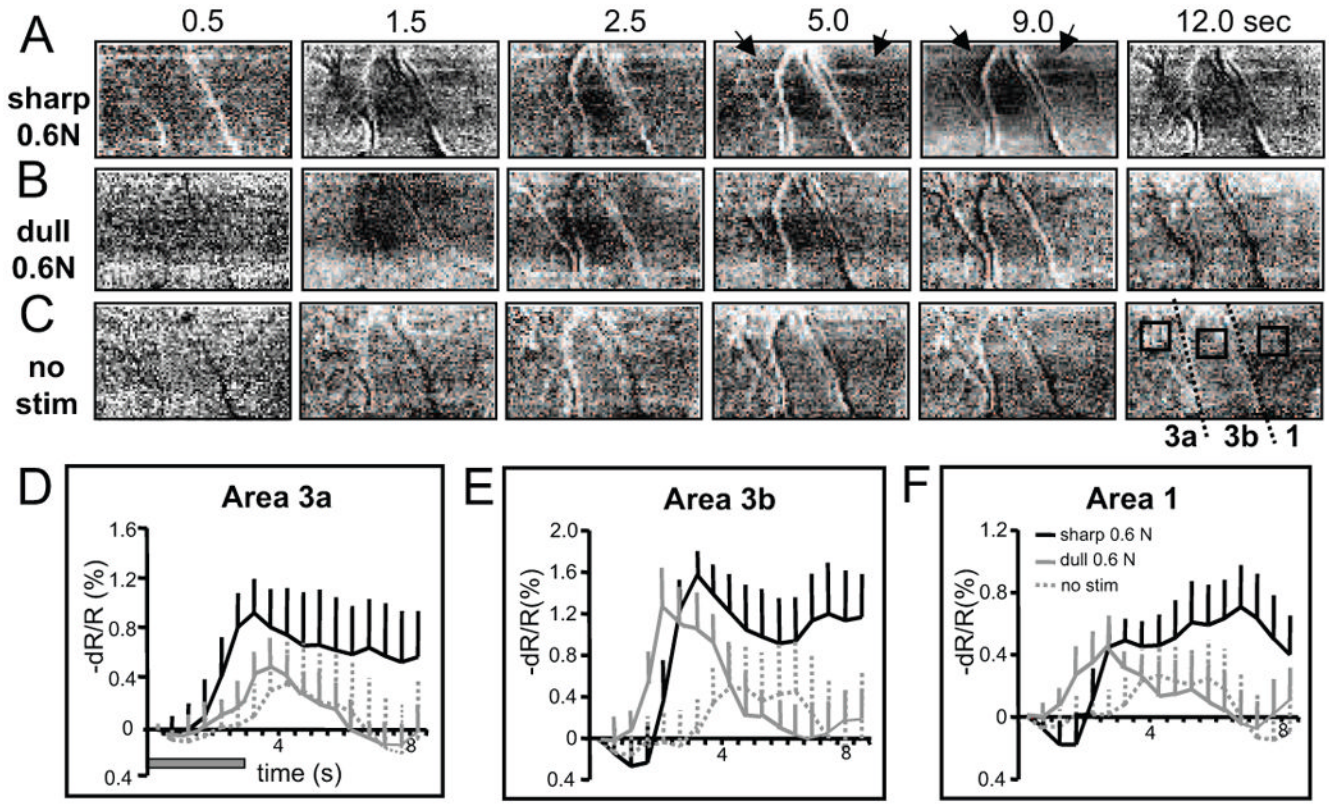

Figure 3.

Optical signal development and temporal profile of the optical signal in SI to nociceptive and innocuous stimuli. Twelve seconds of the temporal development of optical signal observed in the optical maps in areas 3a, 3b and 1 are shown starting before and continuing after the offset of stimulation for stimulation with the 0.2 mm dia (A) or 2 mm probe indentation at 0.6N, and (C) no stimulation. Black arrows indicate points of interest (see text). (D-F). Timecourses of the optical signals taken from regions of interest in areas 3a, 3b and 1 (boxes in the last images of C). Black and gray curves represent changes of light reflectance (-dR/R %) for the three conditions: 0.6N sharp probe (solid black lines), 0.6N dull probe (solid gray lines), and no stimulus (dotted gray lines)).

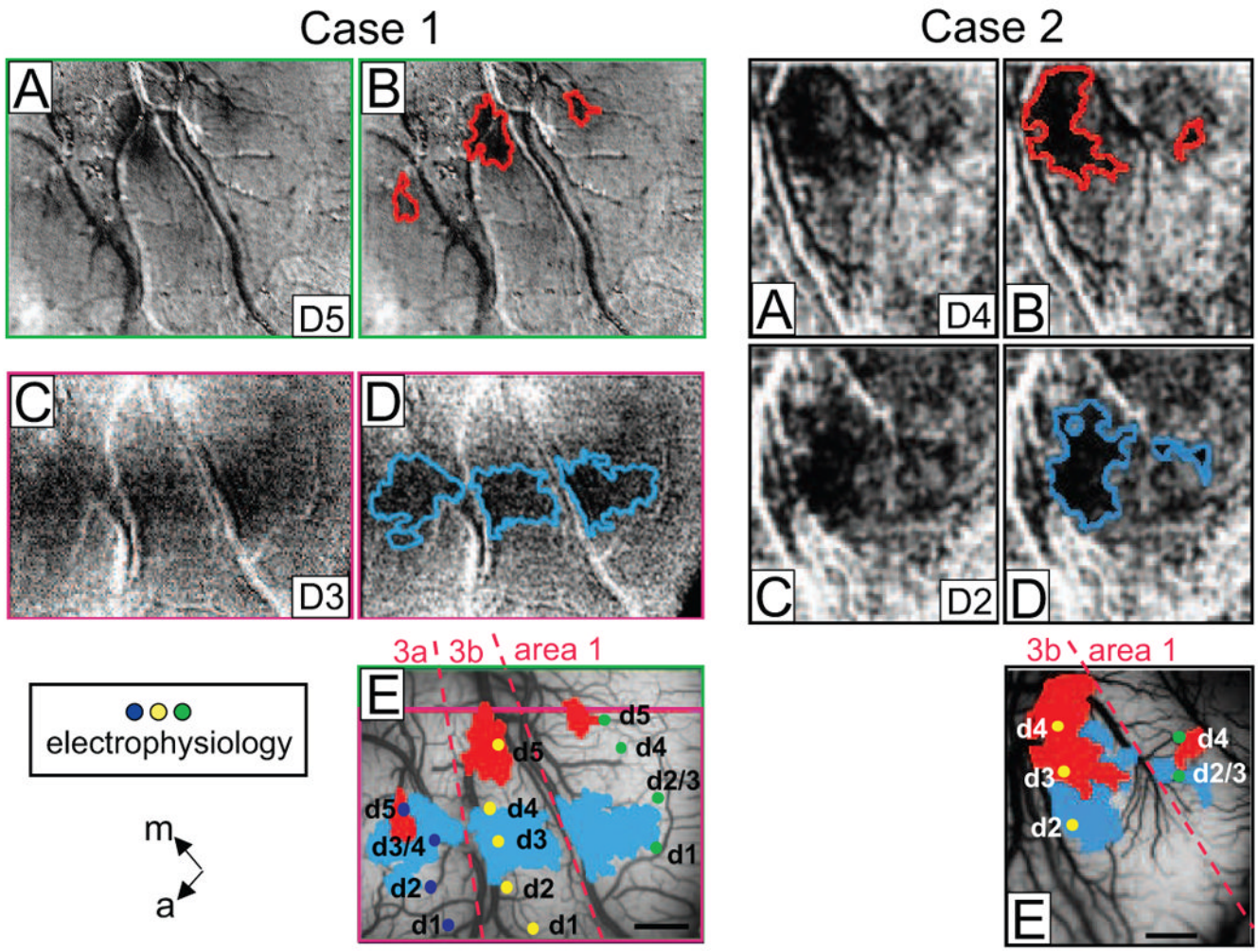

Figure 4.

Topography of response to a mechanical nociceptive stimulus in areas 3a, 3b and 1. Case 1. Left A-E) Presentation of sharp probe on D5 (A, B) and D3 (C, D) evoked 1-1.5 mm activations in areas 3a, 3b and 1. Activation areas are outlined in red (B) and blue (D). E) Activation areas superimposed on the blood vessel map show topographic organizations in areas 3a, 3b and 1. Case 2. Right A-E) Response to the sharp probe indented on digits, D4 (A, B) and D3 (C, D), activation outlines in B and D. E) Superimposition of activation areas on the blood vessel map show topographic organization. Dots: electrophysiological recording sites; labels indicate digit location (d1-d5) of receptive fields. Dashed lines: approximate borders between areas 3a, 3b, and 1. m = medial, a = anterior.

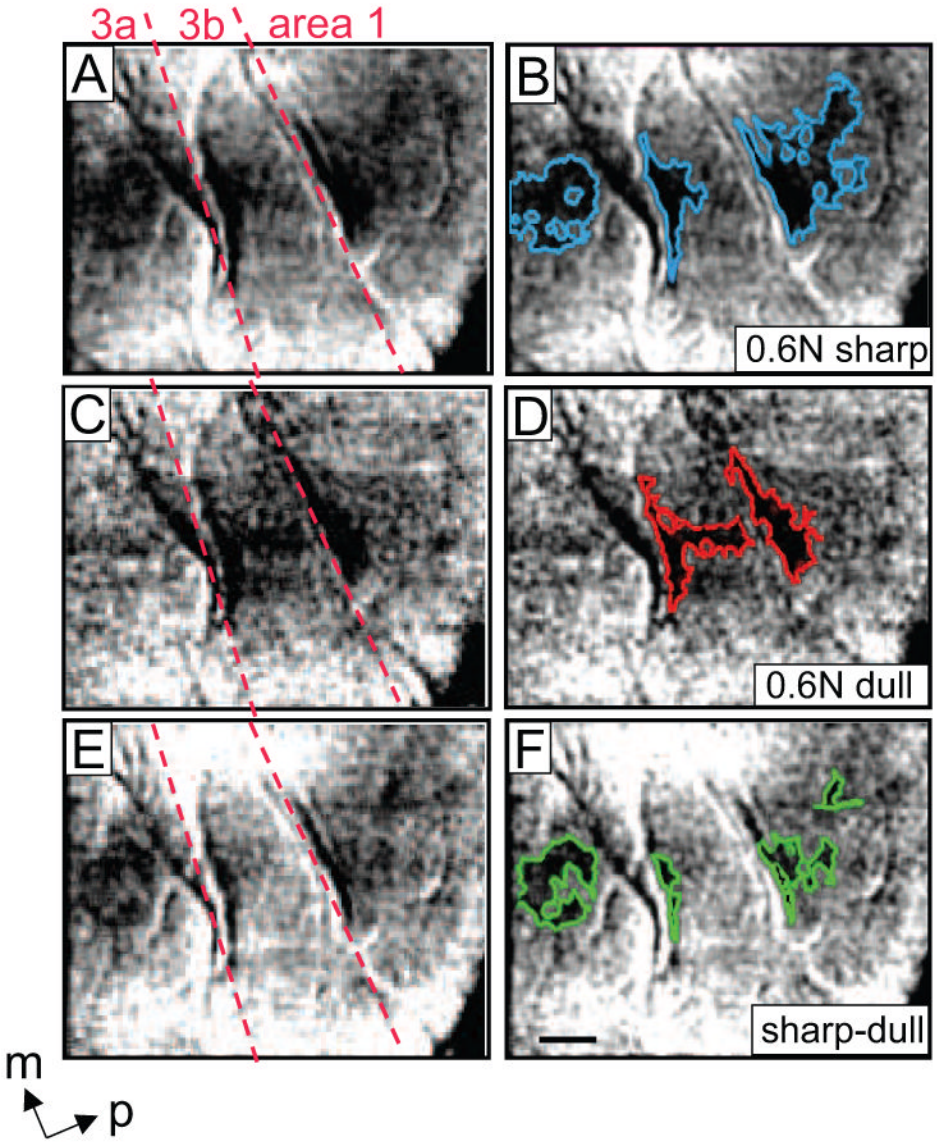

Figure 5.

Different activation patterns were evoked with pressure and the sharp nociceptive probe in SI. Case 1. Moderate (0.6 N) indentations of the 0.2 (nociceptive) and 2 mm (pressure) diameter probes were presented to the D3 distal fingerpad. A-D) Single condition maps showing the focal and spatially distinct activations in areas 3a, 3b and 1 in response to the nociceptive stimulus (A, B) and pressure stimulus (C, D). Activation areas are outlined in blue (B) and red (D). E and F: Subtraction maps (sharp minus dull). C, D) regions exhibiting preferential activation to the sharp probe are outlined in green (F). Nociceptive stimulation produced activation in areas 3a, 3b and 1, whereas pressure elicited activation only in areas 3b and 1. Images were summed over 30 trials. Scale bar = 1 mm. M = medial, p = posterior. Red dotted lines: approximate borders between Areas 3a, 3b, and 1 were determined from the neuronal response properties obtained from electrode mapping SI in this animal.

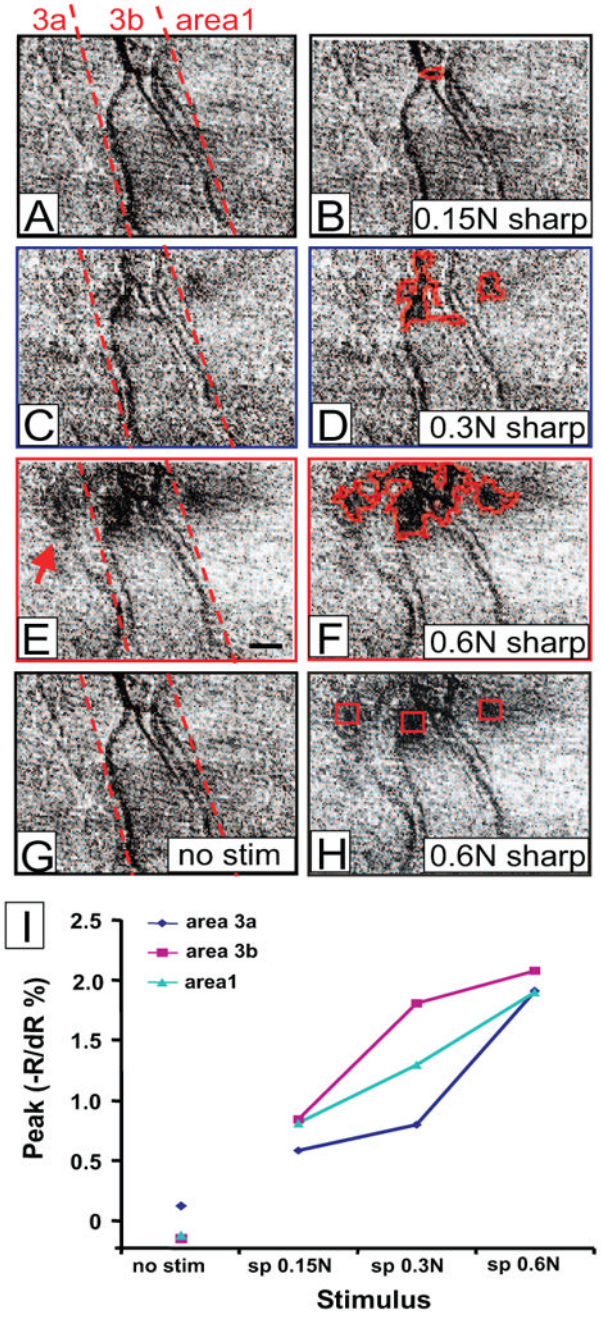

Figure 6.

Cortical responses to increased intensity of mechanical painful stimuli in areas 3a, 3b and 1. Activations evoked with: (A, B) 0.15 N sharp probe, (C, D) 0.3 N sharp probe, and (E, F) 0.6 N sharp probe, and (G) blank. Activations outlined on left (B, D, F). H) Regions of interest (red boxes) in areas 3a, 3b and 1 indicated on (E) map. Dashed lines in A, C, and E: approximate borders of somatosensory areas. (I) Plot of peak reflectance change with indentation force (sharp probe 0.6N: moderately nociceptive; 0.3N: weakly nociceptive, and 0.15 N sharp probe: weak pressure) for areas 3a (blue), 3b(pink) and 1(aqua blue). Scale bar: 1mm.

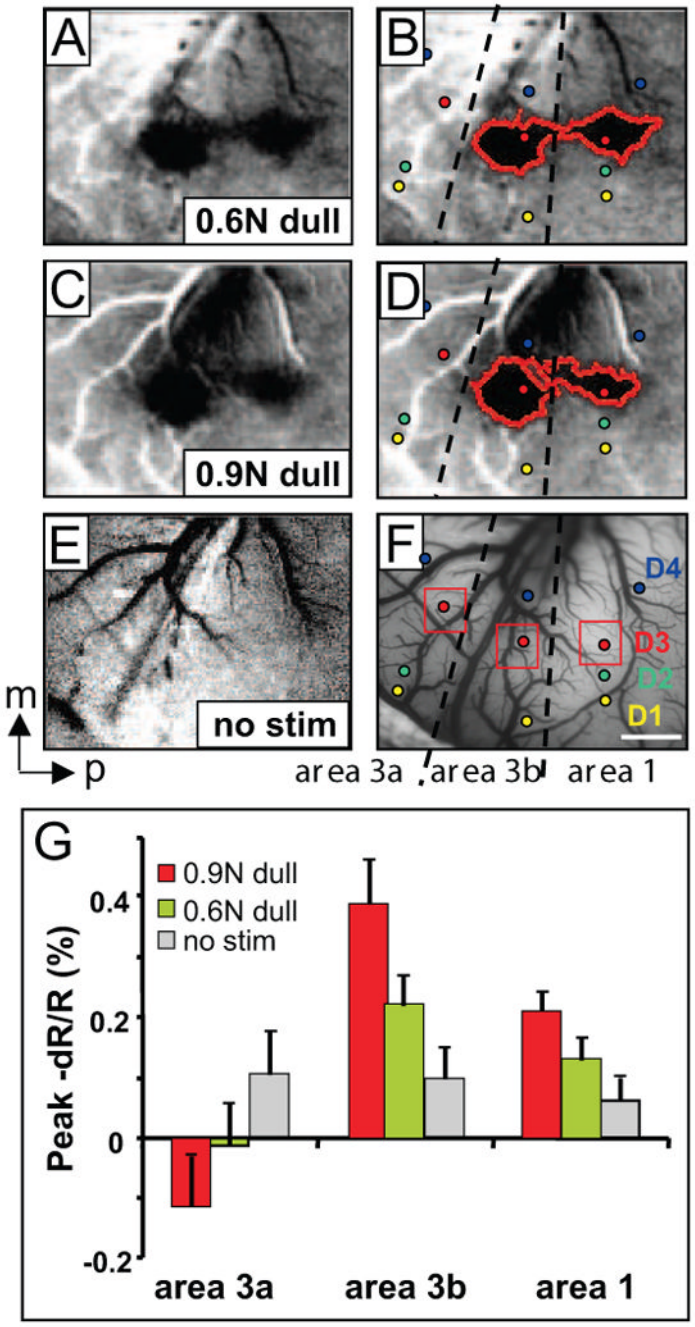

Figure 7.

Cortical responses to increased intensity of pressure stimuli in areas 3a, 3b and 1. Case 3. Activations evoked with: (A, B) 0.6 N pressure stimulus, (C, D) 0.9 N pressure, and (E) no stimulus blank (sum of 30 trials). Activations outlined on left (B, D). F) Regions of interest (red boxes) and electrode penetrations (small circles) superimposed on the blood vessel map. G) Peak change in reflectance signal (mean +/- se) in areas 3a, 3b and 1 to 0.6 N pressure (moderate, green columns), 0.9 N (strong pressure, red columns) and blank (gray columns) in areas 3a, 3b and 1. Dashed lines: approximate borders of areas 3a, 3b and 1. Scale bar: 1mm. m: middle, p: posterior.

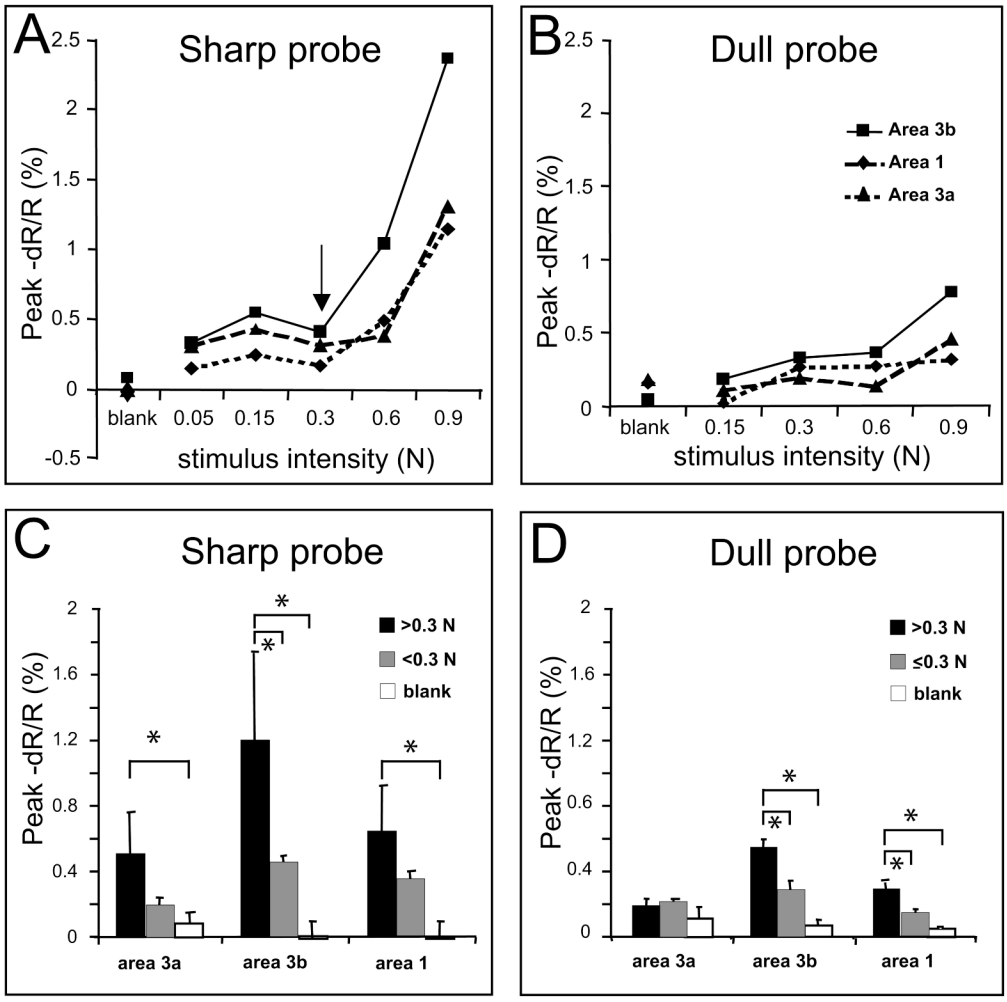

Figure 8.

Comparison of activation amplitudes for various intensities of indentation of the 0.2 and 2 mm diameter probes. A, B) show peak responses to 5 indentation forces with the 0.2 mm diameter probe (A) and 4 indentation forces with the 2 mm in diameter probe (B) in areas 3a (dashed line), 3b (solid) and 1 (dotted). Arrow in A indicates pain threshold. Note the sharp increase in activation with stimulation above 0.3 N. C and D) Amplitude of responses evoked by stimulus intensities above 0.3 N (middle columns) or below 0.3 N (left columns) and blank (right columns) for the 0.2 mm probe (C) and the 2 mm dia probe (D). Note: Below 0.3 N 0.2 mm probe does note evoke pain sensations. * and lines indicate group comparisons, $p<0.05$. E) Peak amplitudes evoked by the 0.2 mm probe (left columns) and 2 mm probe (right columns) averaged over the 4 common intensities. Error lines indicate standard errors.